Received: 13 October 2023 | Accepted: 23 January 2024

DOI: 10.1097/HEP.0000000000000830

ORIGINAL ARTICLE

OPEN

Antagonistic effects of the cytotoxic molecules granzyme B and TRAIL in the immunopathogenesis of sclerosing cholangitis

Mareike Kellerer[1,2] | Sana Javed[1,2,3] | Christian Casar[2,4,5] | Nico Will[2,4] | Laura K. Berkhout[1,2] | Dorothee Schwinge[2,4] | Christian F. Krebs[2,6] | Christoph Schramm[2,4,7] | Katrin Neumann[1,2] | Gisa Tiegs[1,2]

[1]Institute of Experimental Immunology and Hepatology, University Medical Center Hamburg-Eppendorf, Hamburg, Germany

[2]Hamburg Center for Translational Immunology (HCTI), University Medical Center Hamburg-Eppendorf, Hamburg, Germany

[3]Department of Pharmacy, The University of Faisalabad, Pakistan

[4]I. Department of Medicine, University Medical Center Hamburg-Eppendorf, Hamburg, Germany

[5]Bioinformatics Core, University Medical Center Hamburg-Eppendorf, Hamburg, Germany

[6]III. Department of Medicine, University Medical Center Hamburg-Eppendorf, Hamburg, Germany

[7]Martin Zeitz Center for Rare Diseases, University Medical Center Hamburg-Eppendorf, Hamburg, Germany

Correspondence
Gisa Tiegs, Institute of Experimental Immunology and Hepatology, University Medical Center Hamburg-Eppendorf, Martinistr.52, 20246 Hamburg, Germany.
Email: g.tiegs@uke.de

Abstract

Background and Aims: Primary sclerosing cholangitis (PSC) is a chronic cholestatic liver disease characterized by biliary inflammation and fibrosis. We showed an elevated interferon γ response in patients with primary sclerosing cholangitis and in multidrug resistance protein 2-deficient (*Mdr2*$^{-/-}$) mice developing sclerosing cholangitis. Interferon γ induced expression of the cytotoxic molecules granzyme B (GzmB) and TRAIL in hepatic lymphocytes and mediated liver fibrosis in sclerosing cholangitis.

Approach and Results: In patient samples and *Mdr2*$^{-/-}$ mice, we identified lymphocyte clusters with a cytotoxic gene expression profile using single-cell RNA-seq and cellular indexing of transcriptomes and epitopes by sequencing analyses combined with multi-parameter flow cytometry. CD8$^+$ T cells and NK cells showed increased expression of GzmB and TRAIL in sclerosing cholangitis. Depletion of CD8$^+$ T cells ameliorated disease severity in *Mdr2*$^{-/-}$ mice. By using *Mdr2*$^{-/-}$ × *Gzmb*$^{-/-}$ and *Mdr2*$^{-/-}$ × *Tnfsf10*$^{-/-}$ mice, we investigated the significance of GzmB and TRAIL for disease progression in sclerosing cholangitis. Interestingly, the lack of GzmB resulted in reduced cholangiocyte apoptosis, liver injury, and fibrosis. In contrast, sclerosing cholangitis was aggravated in the absence of TRAIL. This correlated with elevated GzmB and interferon γ expression by CD8$^+$ T cells and NK cells enhanced T-cell survival, and increased apoptosis and expansion of cholangiocytes.

Abbreviations: CITE-seq, cellular indexing of transcriptomes and epitopes by sequencing; GzmB, granzyme B; Mdr2, multidrug resistance protein 2; NPC, Nonparenchymal liver cells; PSC, primary sclerosing cholangitis; scRNA-seq, single-cell RNA sequencing; TCR, T-cell receptor; T_{EM}, effector memory T cells; Tnfsf10, tumor necrosis factor superfamily member 10; TRAIL, tumor necrosis factor-related apoptosis-inducing ligand; WT, wild-type.

Mareike Kellerer and Sana Javed shared first authorship. Katrin Neumann and Gisa Tiegs share senior authorship.

Supplemental Digital Content is available for this article. Direct URL citations are provided in the HTML and PDF versions of this article on the journal's website, www.hepjournal.com.

Conclusions: GzmB induces apoptosis and fibrosis in sclerosing cholangitis, whereas TRAIL regulates inflammatory and cytotoxic immune responses, subsequently leading to reduced liver injury and fibrosis.

INTRODUCTION

Primary sclerosing cholangitis (PSC) is a progressive biliary disease characterized by biliary inflammation, fibrosis, cholestasis, end-stage liver disease, and a high risk of malignancy. The rising prevalence of PSC indicates that current medical treatment is poorly effective.[1] Genome-wide association studies implicated T cells and NK cells in the pathology of PSC.[2,3] Since genetic risk factors for autoimmunity have been linked with disease progression,[2] most of the studies addressed the role of $CD4^+$ T cells in PSC.[4–6] However, $CD8^+$ T cells can also contribute to autoimmune diseases.[7] Recently, cytotoxic $CD8^+$ T cells were identified in the livers of patients with PSC,[4,6] but their functional role in biliary disease is less clear.

Multidrug resistance protein 2-deficient (*Mdr2*$^{-/-}$) mice develop sclerosing cholangitis and represent a well-described murine model of PSC that morphologically resembles the histopathological features of patients with PSC.[8] We recently showed an interferon (IFN)γ-induced activation and accumulation of hepatic $CD8^+$ T cells and NK cells expressing the cytotoxic molecules granzyme B (GzmB) and TRAIL in *Mdr2*$^{-/-}$ mice. We further demonstrated that NK cells promote liver injury and fibrosis in sclerosing cholangitis.[9] Since the treatment of *Mdr2*$^{-/-}$ mice with 24-Norursodeoxycholic acid was shown to inhibit $CD8^+$ T-cell differentiation, thereby ameliorating sclerosing cholangitis,[10] this points to a role of $CD8^+$ T cells in disease pathology.

Cytotoxic lymphocytes kill virally infected and malignant cells to ensure immunosurveillance.[11] They degranulate and release GzmB after target cell recognition to induce apoptosis by cleavage of pro-caspase-3.[12] One study has correlated gene expression of GzmB with disease severity of primary biliary cholangitis,[13] suggesting GzmB-mediated liver injury in biliary disease. However, the contribution of GzmB to the disease progression of PSC has not been investigated so far. Cytotoxic lymphocytes can further induce cell death through TRAIL-mediated apoptosis. In humans, TRAIL interacts with 2 death receptors (DR4/TRAIL receptor (R)1 and DR5/TRAIL-R2), whereas mice express mDR5/mTRAIL-R.[14] TRAIL has also been described as a negative regulator of immune responses, thereby preventing autoimmune disorders.[14,15] TRAIL-deficient (tumor necrosis factor superfamily member 10 [*Tnfsf10*$^{-/-}$]) mice and mice lacking mDR5 were protected from acute liver injury, including acute biliary disease.[16–19] Treatment of C57BL/6 mice with an agonistic anti-DR5 antibody induced acute sclerosing cholangitis. Since cholangiocytes of patients with PSC showed increased expression of DR5, this argues for TRAIL-dependent killing of these cells.[18] In contrast, the lack of mDR5 in *Mdr2*$^{-/-}$ mice resulted in more severe chronic sclerosing cholangitis.[20]

In this study, we investigated the role of GzmB-mediated and TRAIL-mediated lymphocyte cytotoxicity for the progression of PSC. We showed that $CD8^+$ T cells and GzmB induced apoptosis in cholangiocytes, thereby aggravating sclerosing cholangitis. In contrast, TRAIL ameliorated disease severity by limiting lymphocyte survival, cytotoxicity, and IFNγ expression as well as by regulating apoptosis and proliferation of cholangiocytes. Thus, we identified GzmB as a cytotoxic mediator of sclerosing cholangitis, whereas TRAIL exerts immunosuppressive functions by regulating cytotoxic and inflammatory lymphocyte responses.

METHODS

Mice

Mdr2$^{-/-}$ mice (C57BL/6.129P2-Abcb4^{tm1Bor}) were provided by Daniel Goldenberg (Goldyne Savad Institute of Gene Therapy, Hadassah-Hebrew University Medical Centre, Jerusalem, Israel). *Gzmb*$^{-/-}$ mice (C57BL/6.129S2-Gzmb^{tm1Ley}/J) were provided by Wei Du (Department of Immunology, Roswell Park Cancer Institute, Buffalo, NY) and *Tnfsf10*$^{-/-}$ mice (C57BL/6.129S7-Tnfsf10^{tm1Sdg}) were obtained from Amgen (Thousand Oaks, CA, USA) by transfer agreement (MTA #2011566296). *Mdr2*$^{-/-}$x*Rag1*$^{-/-}$ (B6.129P2-Abcb4t^{m1Bor}x B6.129S7-Rag1^{tm1Mom}/J), *Mdr2*$^{-/-}$ × *Gzmb*$^{-/-}$ and *Mdr2*$^{-/-}$ × *Tnfsf10*$^{-/-}$ mice were generated by crossbreeding of the respective single knockouts. All mice were bred in the animal facility of the University Medical Center Hamburg-Eppendorf (UKE; Hamburg, Germany) according to the Federation of European Laboratory Animal Science Association guidelines. All mice received human care. The experiments were approved by the institutional review board (Behörde für Gesundheit und Verbraucherschutz, Hamburg, Germany) and carried out according to the German animal protection law. Mice were housed in IVC cages under controlled conditions (22°C, 55% humidity, and

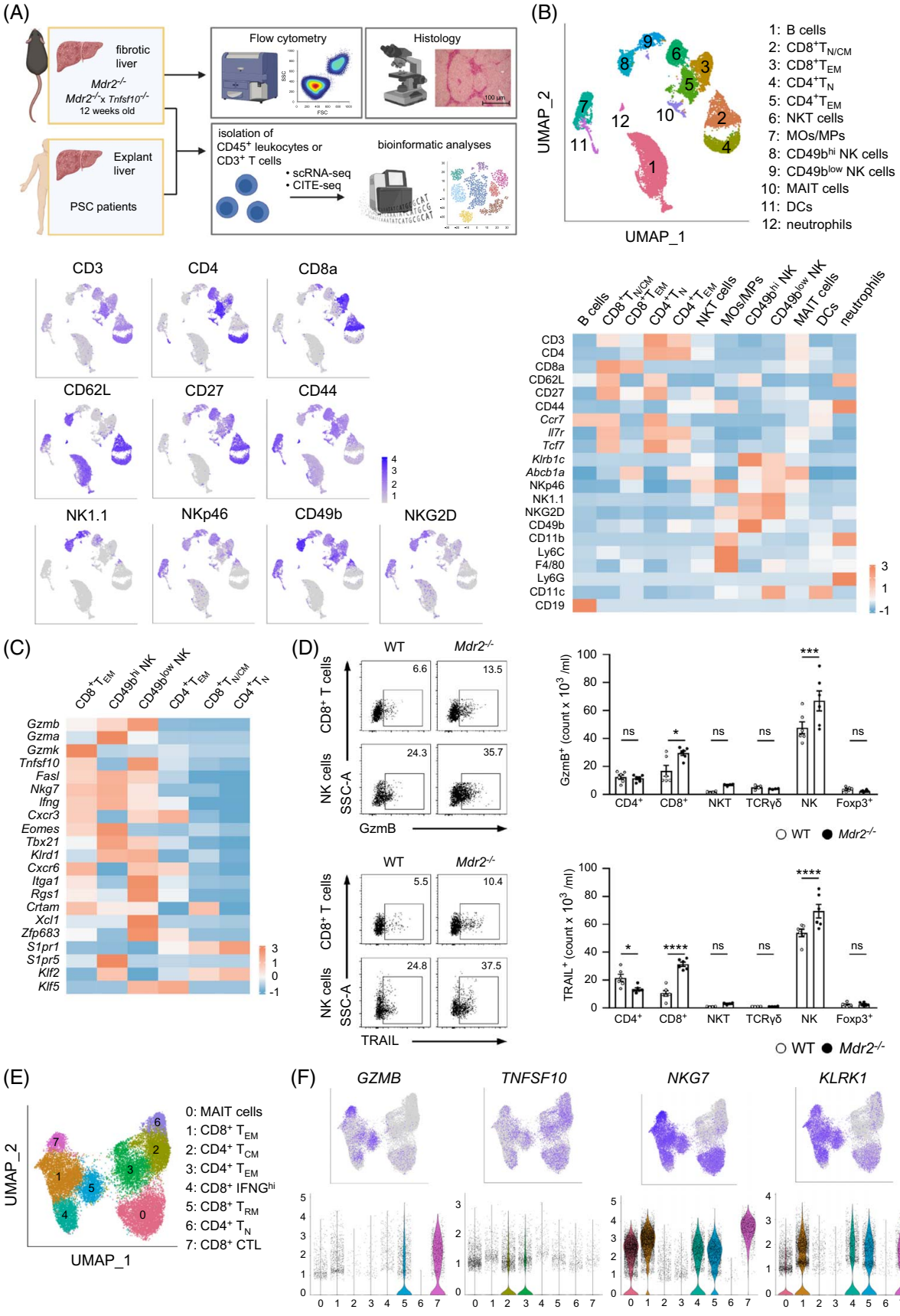

FIGURE 1 Cytotoxic lymphocyte subsets in PSC. (A) Schematic overview of the study design. (B) UMAP plot shows clustering of CD45$^+$ leukocytes in sclerosing cholangitis. UMAP plots and heat maps show subset defining protein and gene expression. (C) Heat map of genes

defining effector cell function. (D) Expression of TRAIL and GzmB by hepatic T-cell subsets and NK cells was analyzed in 12-week-old Mdr2$^{-/-}$ and WT mice. (E) UMAP plot shows clustering of CD3^{+} T-cell subsets from patients with PSC. (F) UMAP and violin plots depict the expression of genes associated with cytotoxicity within the different T-cell subsets. Mean ± SEM of 1 out of 2 experiments are shown. *$p \leq 0.05$, ***$p \leq 0.001$, ****$p \leq 0.0001$, ns: not significant. Abbreviations: GzmB, granzyme B; Mdr2, multidrug resistance protein 2; MOs/MPs, monocytes/monocyte-derived macrophages; PSC, primary sclerosing cholangitis; UMAP, Uniform Manifold Approximation and Projection; WT, wild-type.

12 hour day-night rhythm) and fed a standard laboratory chow (LASvendi, Altromin, Germany).

Patients

In this study, a published data set from patients with PSC undergoing liver transplantation was used for the analyses.[6]

Animal treatment

Depletion of CD8^{+} T cells was performed in 6-week-old male and female *Mdr2*$^{-/-}$ mice by i.p. injection of an anti-CD8 antibody (0.5 mg/mouse; *InVivo*MAb clone YTS 169.4; BioXCell, Köln, Germany) or an isotype control anti-rat IgG2 antibody (0.5 mg/mouse; *InVivo*Mab clone 2A3; BioXCell) twice a week for 2 weeks. For adoptive transfer experiments, CD8^{+} T cells were isolated from the spleen and lymph nodes of C57BL/6 wild-type (WT) and *Tnfsf10*$^{-/-}$ mice. 2×10^5 WT or *Tnfsf10*$^{-/-}$ CD8^{+} T cells were i.v. injected into *Mdr2*$^{-/-}$×*Rag1*$^{-/-}$ mice, which were analyzed 8 days later.

Isolation of hepatic leukocytes and antibody staining for sequencing

Nonparenchymal liver cells (NPCs) were isolated from livers of 12 weeks old *Mdr2*$^{-/-}$ and *Mdr2*$^{-/-}$ × *Tnfsf10*$^{-/-}$ mice by Percoll density gradient centrifugation and stained with a LIVE/DEAD Fixable Staining Kit and an anti-CD45 antibody (30-F11, PerCP, BioLegend). At the same time, NPCs were stained with antibodies for cellular indexing of transcriptomes and epitopes by sequencing (CITE-seq; TotalSeq-B Mouse Universal Cocktail, TotalSeq-B anti-mouse CD314, TotalSeq-B anti-mouse CD335; all BioLegend) for epitope detection. Subsequently, CD45^{+} leukocytes were isolated by FACS.

Single-cell RNA sequencing

To perform single-cell RNA sequencing (scRNA-seq), FACS-sorted CD45^{+} hepatic leukocytes were subjected to droplet-based single-cell analysis using the Chromium Single Cell 5′ Reagent Kits v2 chemistry according to the manufacturer's instructions (Chromium, 10x Genomics, Pleasanton, CA). Gene and protein expression libraries were sequenced on a NovaSeq 6000 System (Novogene, Cambridge, UK).

Alignment, quality control, and pre-processing of scRNA-seq data

Cell Ranger (version 7.10; 10X Genomics) was used to produce combined feature-barcode matrices for the scRNA- and CITE-seq data by aligning the RNA reads to the mouse reference genome (refdata-gex-mm10-2020-A). Cellbender (version 0.3.0)[21] was used to remove ambient RNA and reduce noise in the CITE-seq assay. Subsequently, solo (version 1.3)[22] was used to remove possible cell doublets. The data was further processed with R (version 4.2.2, R Core Team). For quality control and downstream processing, Seurat (version 4.3.0)[23] was used. We kept cells for the analysis that contained between 700 and 4500 genes, between 1000 and 20,000 UMIs, and mitochondrial gene expression below 6%. We used Seurat SCTransform to normalize the RNA expression and centered log-ratio transformation from NormalizeData for the CITE-Seq data.

Dimensionality reduction and clustering

Since we did not observe obvious batch effects, we merged the count matrices of all samples and performed principal component analysis on the combined data. We used the first 12 principle components, as estimated by the maxLikGlobalDimEst function from the intrinsicDimension package, for KNN graph construction and Uniform Manifold Approximation and Projection. To find cell clusters, we used the Leiden algorithm with a resolution of 0.2. Cluster markers were calculated with FindAllMarkers using logistic regression and the donor information as a latent variable. Gene expression differences between *Mdr2*$^{-/-}$ and *Mdr2*$^{-/-}$ × *Tnfsf10*$^{-/-}$ mice within each cluster were calculated with the run_de function from the package Libra (version 1.0.0)[24] using the single-cell mode and the Wilcoxon Rank-Sum test. An adjusted *p*-value of less than 0.05 was considered statistically significant.

Flow cytometry

NPCs were isolated from murine livers by Percoll density gradient centrifugation. Erythrocytes were lysed

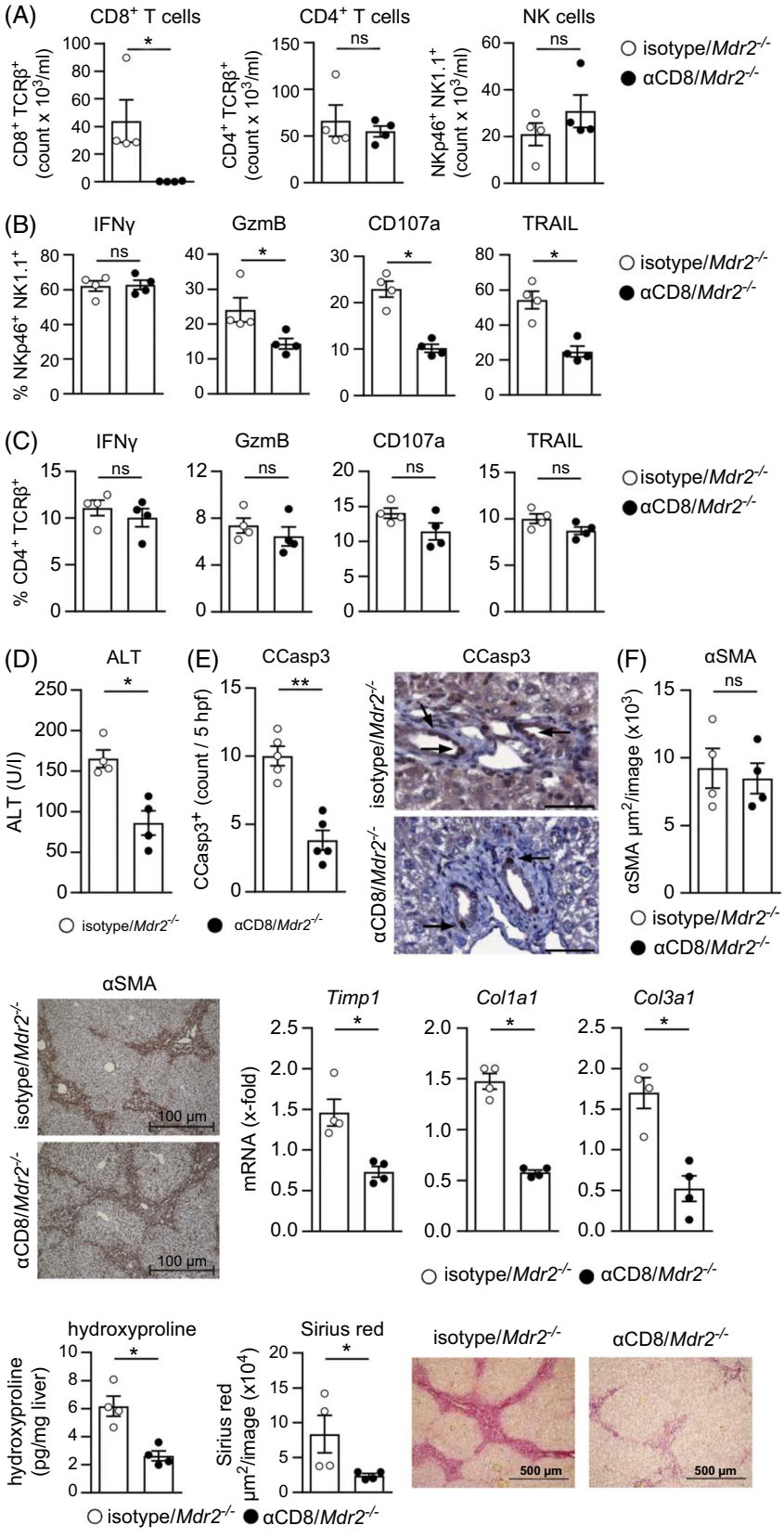

FIGURE 2 CD8⁺ T cells aggravate sclerosing cholangitis. (A) Six-weeks old Mdr2$^{-/-}$ mice were treated with an anti-CD8α antibody or isotype control twice a week for 2 weeks. Numbers of hepatic CD8⁺ and CD4⁺ T cells and NK cells were analyzed. (B) The phenotype of hepatic NK cells and (C) CD4⁺ T cells was analyzed. (D) Plasma ALT levels were determined. (E) CCasp3 was stained in liver sections, and CCasp3-expressing cholangiocytes were counted. Arrows mark CCasp3⁺ cholangiocytes. Bars represent 50 µm. (F) αSMA staining was quantified in liver sections.

Expression of Timp1, Col1a1, and Col3a1 was determined in antibody-treated mice and normalized to the isotype control. Hydroxyproline levels were assessed in liver tissue, and Sirius red staining was quantified in liver sections. Mean ± SEM of 1 out of 2 experiments are shown. *$p \leq 0.05$, **$p \leq 0.01$, ns: not significant. Abbreviations: CCasp3, cleaved caspase-3; Col1a1, collagen type I alpha 1 chain; Col3a1, collagen type 3 alpha 1 chain; αSMA, α-smooth muscle actin.

with NH_4Cl. NPCs were incubated with an anti-CD16/32 antibody (93; BioLegend) before antibody staining to prevent unspecific binding. LIVE/DEAD Fixable Staining Kits (ThermoFisher Scientific) were used to exclude dead cells. NPCs were stained with the fluorochrome-labelled antibodies listed in Supplemental Table S1, http://links.lww.com/HEP/I333. For intracellular staining, NPCs were re-stimulated with phorbol myristate acetate (20 ng/ml) and ionomycin (1 μg/ml) for 4 hours with the addition of brefeldin A (1 μg/ml; all Sigma Aldrich) and monensin (2 μM; BioLegend) after 30 min. The anti-CD107a antibody (1D4B; FITC; BioLegend) was added to the medium. After surface and Live/Dead staining, NPCs were fixed using the Transcription Factor Staining Buffer Set (ThermoFisher Scientific) and incubated in Permeabilization buffer with antibodies specific to IFNγ (XMG1.2; PE-CF594; BD Biosciences), GzmB (GB11; Pacific Blue; BioLegend) and Foxp3 (MF-14; PerCP-Cy5.5, FITC; ThermoFisher Scientific). Analyses were done using a BD LSRFortessa Cell Analyzer (BD Biosciences). Antibodies used for cell surface staining for flow cytometry are given in Supplemental Table S1, http://links.lww.com/HEP/I333.

Immunohistochemistry

To identify proliferating cholangiocytes, 3 μm paraffin-embedded liver sections were stained with an anti-Ki-67 antibody (polyclonal, Abcam, Cambridge, UK). After incubation with a biotin-conjugated secondary antibody (Agilent Technologies, Santa Clara, CA), the ZytoChem-Plus AP Polymer-Kit (Zytomed Systems, Berlin, Germany) was used for Ag detection. To identify apoptotic cholangiocytes, liver sections were stained with an anti-cleaved caspase 3 antibody (ThermoFisher Scientific). After incubation with goat anti-rabbit-HRP secondary antibody (ThermoFisher Scientific), liver sections were stained with DAB+ substrate (Agilent Technologies). Ki-67$^+$ and CCasp3$^+$ cholangiocytes were counted in 5 high-power fields (each 125 μm^2) randomly defined in liver tissue.

Statistical analysis

Statistical analyses were performed using GraphPad Prism 7 software (GraphPad Software, San Diego, CA). All data are presented as mean ± SEM. For comparisons between 2 groups, a nonparametric Mann-Whitney *U* test and for more than 2 groups, a one-way ANOVA with Tukey's post hoc test was used. A *p*-value of less than 0.05 was considered statistically significant with the following ranges *$p \leq 0.05$, **$p \leq 0.01$, ***$p \leq 0.001$, ****$p \leq 0.0001$.

Additional materials and methods are described in the Supplemental Materials and Methods, http://links.lww.com/HEP/I333.

RESULTS

Cytotoxic lymphocyte subsets in livers of mice with sclerosing cholangitis and patients with PSC

To understand the functional relevance of cytotoxic T-cell subsets in biliary disease, we isolated CD45$^+$ leukocytes from livers of 12-week-old *Mdr2*$^{-/-}$ mice and subjected them to scRNA-seq and CITE-seq (Figure 1A). At this age, *Mdr2*$^{-/-}$ mice developed sclerosing cholangitis characterized by elevated plasma alanine transaminase levels, increased expression of fibrosis-associated genes, including *Timp1*, collagen type I alpha 1 chain, and collagen type 3 alpha 1 chain, collagen deposition assessed by elevated levels of hydroxyproline and Sirius red staining, and enhanced expression of the myofibroblast marker α-smooth muscle actin (Supplemental Fig. S1A-E, http://links.lww.com/HEP/I333). We included about 17,000 cells from 6 mice in the analyses and applied principal component analysis on variably expressed genes and proteins across CD45$^+$ leukocytes to generate Uniform Manifold Approximation and Projection. Based on subset signatures, we identified 12 clusters within the hepatic leukocytes, including CD3$^+$ CD44$^+$ CD27$^+$ CD62L$^-$ *Ccr7*$^-$ effector memory T cells (T_{EM}), CD3$^+$ CD44$^-$ CD27$^+$ CD62L$^+$ *Ccr7*$^+$ naïve T cells, and CD49b^{hi} and CD49b^{low} NK1.1$^+$ NKp46$^+$ CD3$^-$ NK cells (Figure 1B). In sclerosing cholangitis, CD8$^+$ T_{EM} expressed genes associated with cytotoxicity (*Gzmb*, *Gzmk*, *Tnfsf10*, *Fasl*, *Nkg7*, and *Eomes*), inflammation (*Ifng* and *Tbx21*) and tissue residency (*Cxcr6*, *Itga1*, *Rgs1*, and *Crtam*), whereas genes linked with tissue egress (*S1pr1*, *S1pr5*, *Klf2*, and *Klf5*) were less expressed. We did not detect cytotoxic CD4$^+$ T cells in the livers of *Mdr2*$^{-/-}$ mice (Figure 1C). We identified 2 NK cell subsets, which differ in their expression of CD49b (Figure 1B). CD49b^{hi} and CD49b^{low} NK cells expressed *Gzma*, *Gzmb*, *Fasl*, *Nkg7*, and *Ifng*. While CD49^{hi} NK cells expressed genes crucial for recirculation and tissue egress, CD49^{low} NK cells expressed genes associated with tissue residency, particularly *Zfp683*. CD49b^{low} NK cells also expressed *Tnfsf10*, whereas we did not determine *Tnfsf10* in CD49b^{hi} NK cells (Figure 1C).

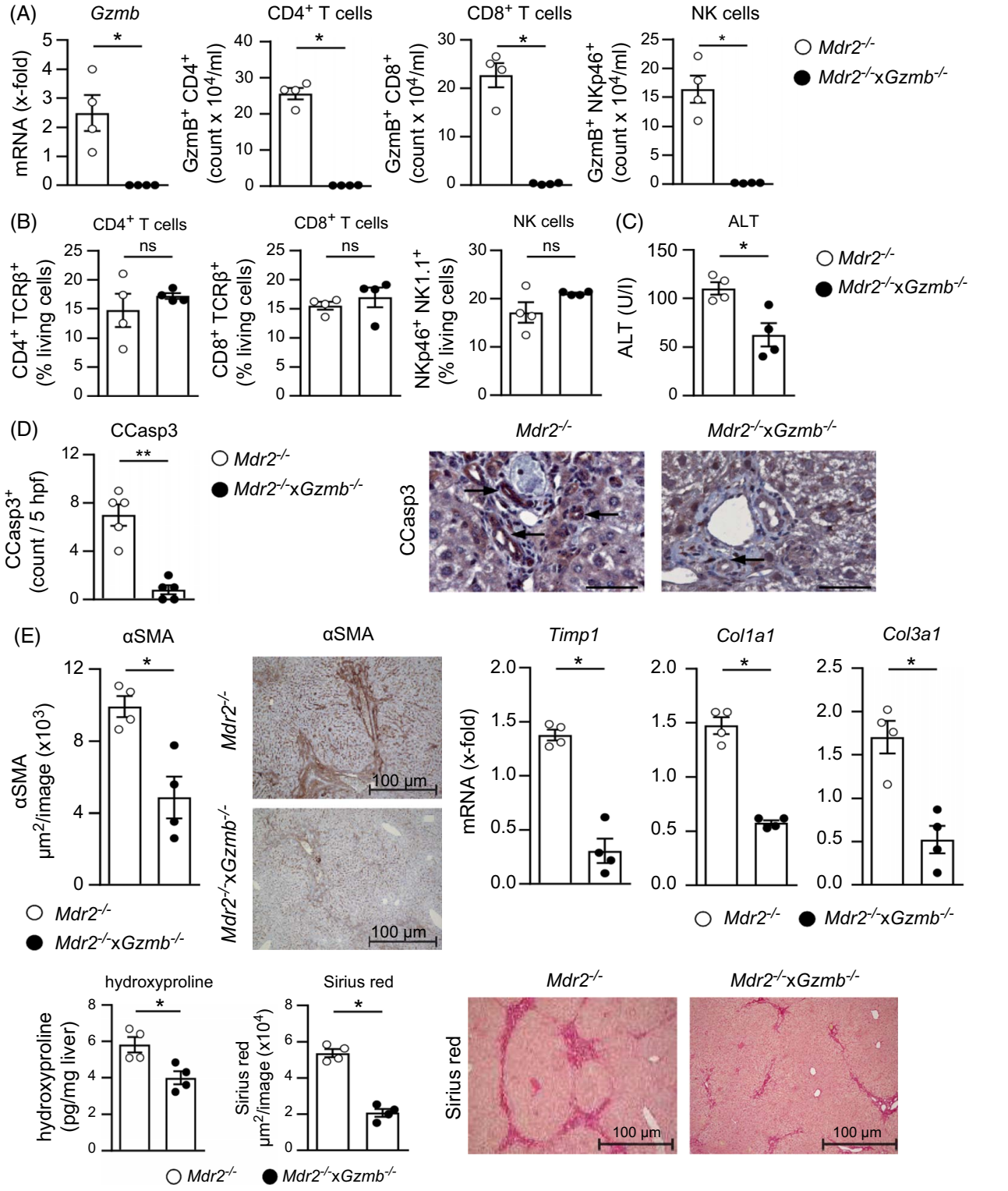

FIGURE 3 GzmB aggravates sclerosing cholangitis. (A) Hepatic Gzmb mRNA expression and GzmB expression in hepatic T cells and NK cells in 12-week-old Mdr2$^{-/-}$ × Gzmb$^{-/-}$ and Mdr2$^{-/-}$ mice are shown. (B) Frequencies of hepatic CD4$^+$ and CD8$^+$ T cells and NK cells were analyzed. (C) Plasma ALT levels were determined. (D) CCasp3 was stained in liver sections, and CCasp3-expressing cholangiocytes were counted. Arrows mark CCasp3$^+$ cholangiocytes. Bars represent 50 µm. (E) αSMA staining was quantified in liver sections. Hepatic expression of Timp1, Col1a1, and Col3a1 was determined in Mdr2$^{-/-}$ × Gzmb$^{-/-}$ mice and normalized to Mdr2$^{-/-}$ mice. Hydroxyproline levels were assessed in liver tissue, and Sirius red staining was quantified in liver sections. Mean ± SEM of 1 out of 3 experiments are shown. *$p \leq 0.05$, **$p \leq 0.01$, ns: not significant. Abbreviations: CCasp3, cleaved caspase-3; Col1a1, collagen type I alpha 1 chain; Col3a1, collagen type 3 alpha 1 chain; GzmB, granzyme B; Mdr2, multidrug resistance protein 2; αSMA, α-smooth muscle actin.

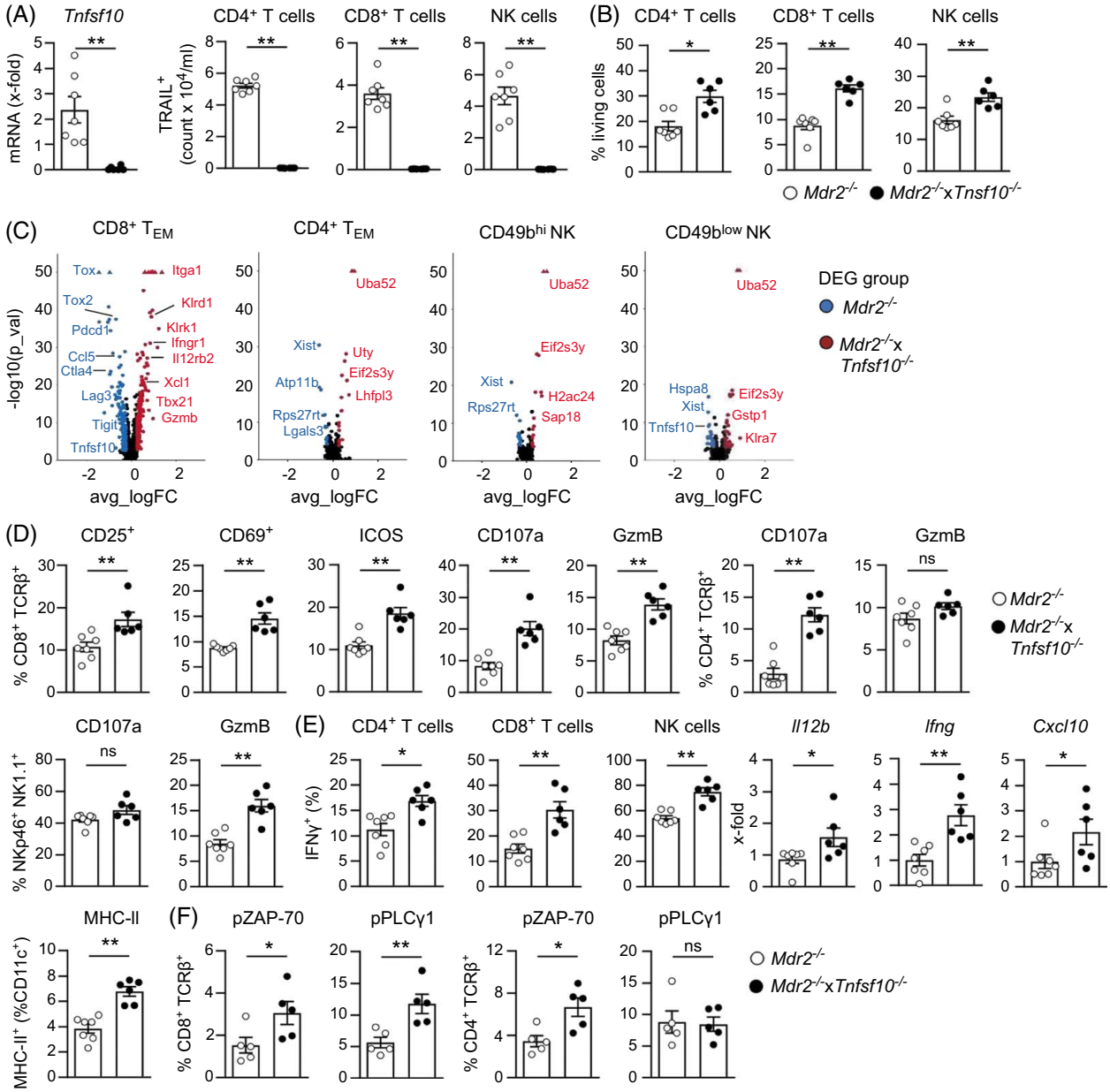

FIGURE 4 TRAIL regulates cytotoxic and inflammatory lymphocytes in sclerosing cholangitis. (A) Tnfsf10 mRNA expression in liver tissue and TRAIL expression in hepatic T cells and NK cells in 12 weeks old Mdr2$^{-/-}$ × Tnfsf10$^{-/-}$ and Mdr2$^{-/-}$ mice are shown. (B) Frequencies of hepatic CD4$^+$ and CD8$^+$ T cells and NK cells were analyzed. (C) Volcano plots depict the most upregulated genes in lymphocyte subsets in Mdr2$^{-/-}$ × Tnfsf10$^{-/-}$ compared to Mdr2$^{-/-}$ mice. (D) The phenotype of hepatic CD8$^+$ T cells, CD4$^+$ T cells, and NK cells is shown. (E) Expression of IFNγ in hepatic lymphocytes was analyzed. Hepatic mRNA expression was determined in Mdr2$^{-/-}$ × Tnfsf10$^{-/-}$ mice and normalized to Mdr2$^{-/-}$ mice. The frequency of hepatic MHC-II$^+$ DCs is shown. (F) Expression of pZAP-70 and pPLCγ1 was analyzed in hepatic CD8$^+$ T cells and CD4$^+$ T cells. Mean ± SEM of 1 out of 3 experiments are shown. *$p \leq 0.05$, **$p \leq 0.01$, ns: not significant. Abbreviations: Mdr2, multidrug resistance protein 2; PLCγ1, phospholipase Cγ1; pZAP, phosphorylated; Tnfsf10, tumor necrosis factor superfamily member 10; ZAP-70, zeta chain-associated protein kinase 70.

We analyzed the protein expression of GzmB and TRAIL by hepatic lymphocytes in sclerosing cholangitis. We showed expression of both, particularly in CD4$^+$ and CD8$^+$ T cells and NK cells. However, only the numbers of GzmB-expressing and TRAIL-expressing CD8$^+$ T cells and NK cells were elevated in *Mdr2*$^{-/-}$ compared to age-matched C57BL/6 WT mice (Figure 1D, Supplemental Fig. S1F, http://links.lww.com/HEP/I333).

We further investigated a previously published data set from patients with PSC undergoing liver transplantation. Here, scRNA-seq and CITE-seq were done with CD3$^+$ T cells isolated from the livers of these patients.[6] We included 25,642 CD3$^+$ T cells from 10 patients with PSC in our analysis and identified 8 clusters such as cytotoxic CD8$^+$ *GZMB*^{hi} CCR7^{low} *SELL*^{low} effector T cells (CD8$^+$ CTLs), *CD27*^{hi} *CCR7*^{low} *SELL*^{low} T_{EM}, CD8$^+$ *CD69*^{hi} CCR7^{low} *SELL*^{low} *ZNF683*^{hi} tissue-resident

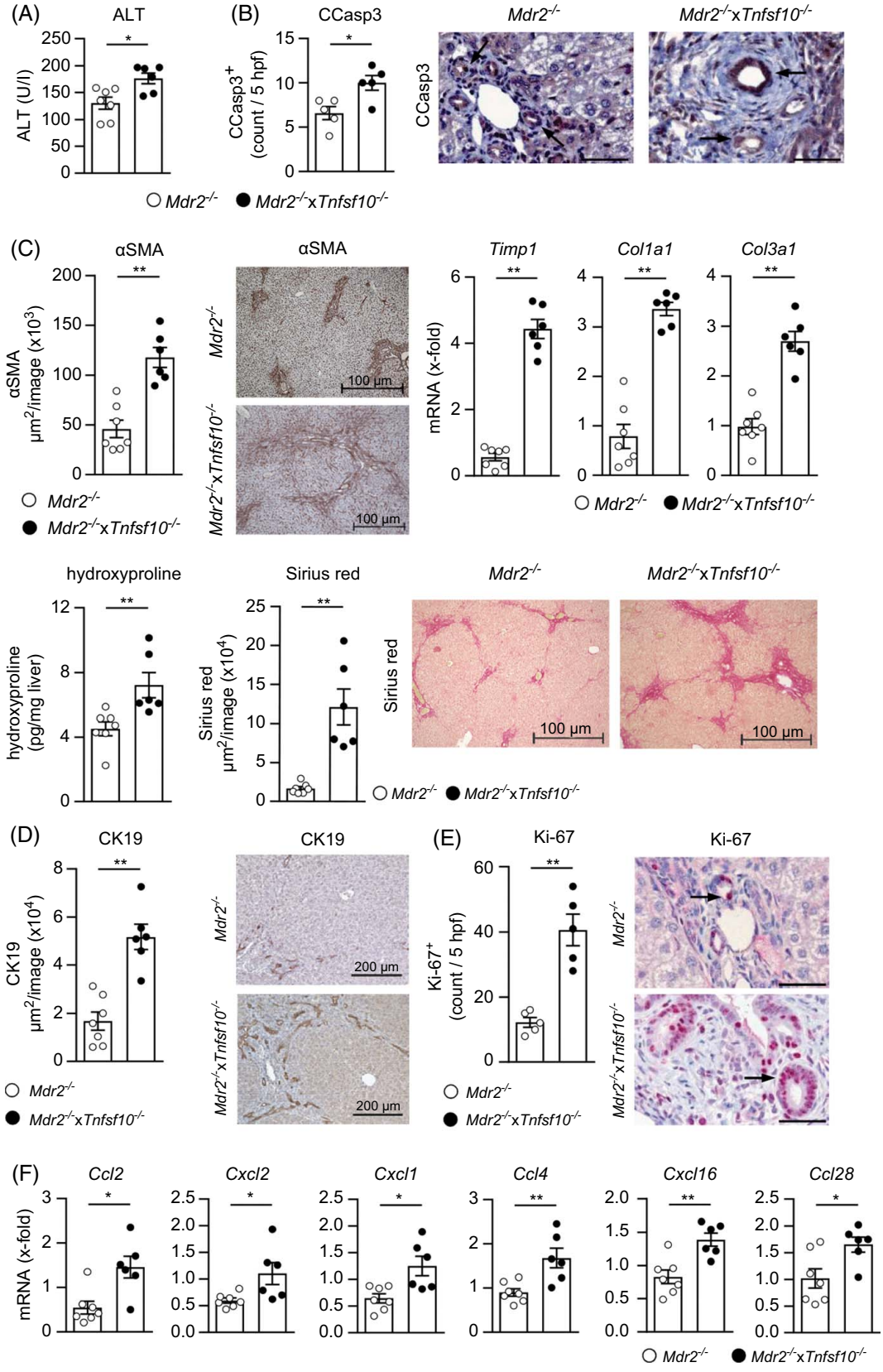

FIGURE 5 TRAIL controls cholangiocyte apoptosis and proliferation in sclerosing cholangitis. (A) Plasma ALT levels were determined in 12-week-old Mdr2$^{-/-}$ × Tnfsf10$^{-/-}$ and Mdr2$^{-/-}$ mice. (B) CCasp3 was stained in liver sections, and CCasp3-expressing cholangiocytes were counted. Arrows mark CCasp3^{+} cholangiocytes. Bars represent 50 µm. (C) αSMA staining was quantified in liver sections. Hepatic expression of Timp1, Col1a1, and Col3a1 was determined in Mdr2$^{-/-}$ × Tnfsf10$^{-/-}$ mice and normalized to Mdr2$^{-/-}$ mice. Hydroxyproline levels were assessed in liver

tissue, and Sirius red and (D) CK19 staining was quantified in liver sections. (E) Ki-67 was stained in liver sections, and Ki-67-expressing cholangiocytes were counted. Arrows mark Ki-67$^+$ cholangiocytes. Bars represent 50 μm. (F) Liver mRNA expression was analyzed in Mdr2$^{-/-}$ × Tnfsf10$^{-/-}$ mice and normalized to Mdr2$^{-/-}$ mice. Mean ± SEM of 1 out of 3 experiments are shown. *$p \leq 0.05$, **$p \leq 0.01$, ns: not significant. Abbreviations: CCasp3, cleaved caspase-3; Col1a1, collagen type I alpha 1 chain; Col3a1, collagen type 3 alpha 1 chain; Mdr2, multidrug resistance protein 2; Tnfsf10, tumor necrosis factor superfamily member 10; αSMA, α-smooth muscle actin.

memory T cells (CD8$^+$ T_{RM}) and *KLRB1*^{hi} *CCR6*^{hi} *IL7R*^{hi} *IL23R*^{hi} CD160^{hi} mucosal-associated invariant T cells (Figure 1E, Supplemental Fig. S2A-C, http://links.lww.com/HEP/I333). We determined the selective expression of *GZMB* by CD8$^+$ CTLs and CD8$^+$ T_{RM}, while other genes associated with cytotoxicity, including *KLRK1* and *NKG7,* were also expressed by other CD8$^+$ T-cell subsets and mucosal-associated invariant T cells. In contrast, low expression of *TNFSF10* was detected within all T-cell subsets (Figure 1F). Thus, hepatic cytotoxic lymphocyte subsets were present in murine and human PSC.

Reduced sclerosing cholangitis and NK cell cytotoxicity in the absence of CD8$^+$ T cells

To assess the role of CD8$^+$ T cells in the induction of hepatic cell death and fibrosis in sclerosing cholangitis,

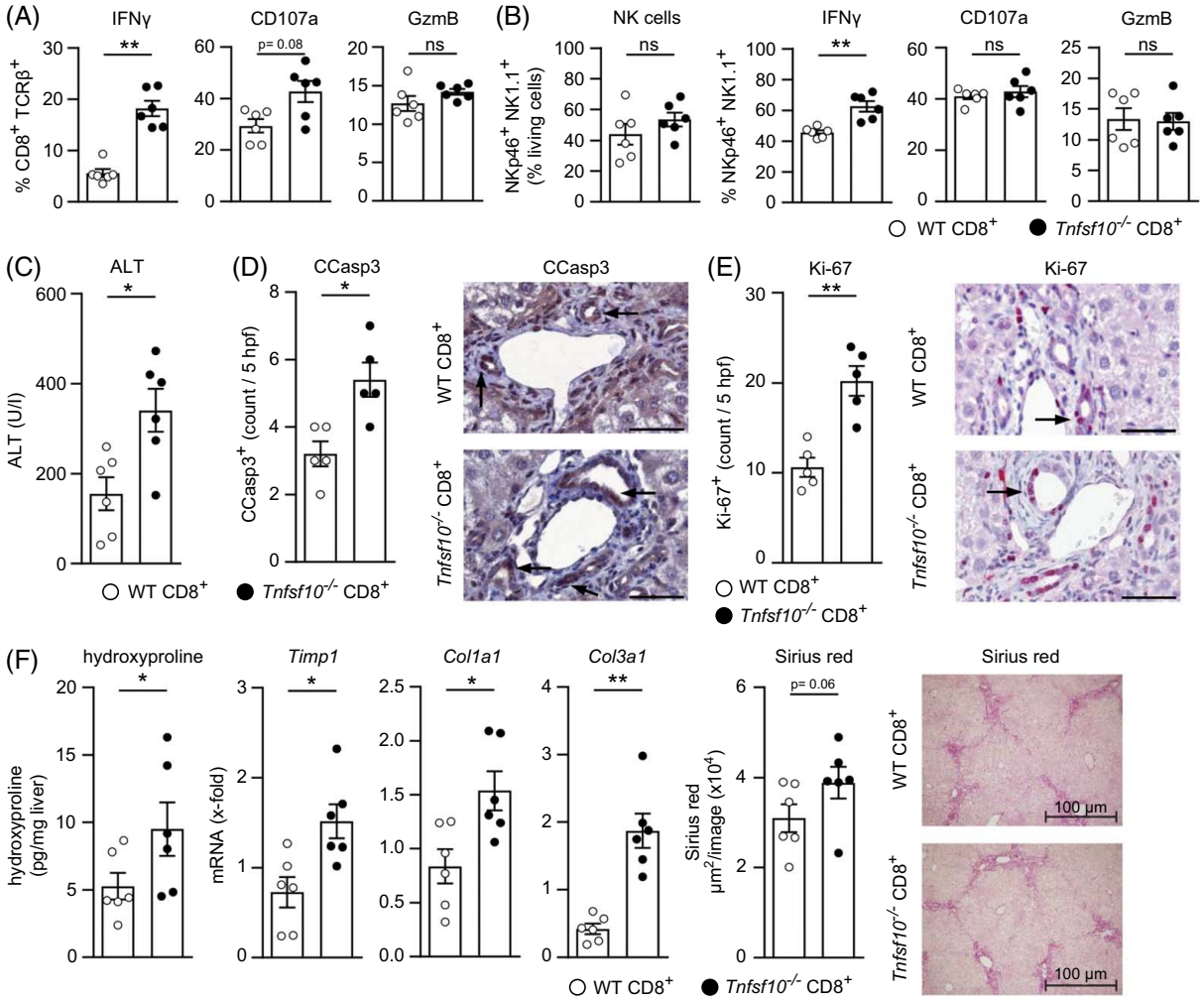

FIGURE 6 Regulation of inflammatory lymphocytes by CD8$^+$ T-cell-derived TRAIL. (A) CD8$^+$ T cells from Tnfsf10$^{-/-}$ and WT mice were transferred into 10-week-old Mdr2$^{-/-}$ × Rag1$^{-/-}$ mice, that were analyzed 8 days later. The phenotype of transferred CD8$^+$ T cells and (B) endogenous NK cells was analyzed. (C) Plasma ALT levels were determined. (D) CCasp3 was stained in liver sections, and CCasp3-expressing cholangiocytes were counted. Arrows mark CCasp3$^+$ cholangiocytes. Bars represent 50 μm. (E) Liver sections were stained with Ki-67, and Ki-67-expressing cholangiocytes were counted. Arrows mark Ki-67$^+$ cholangiocytes. Bars represent 50 μm. (F) Hydroxyproline levels were assessed in liver tissue. Hepatic mRNA expression was analyzed after the transfer of Tnfsf10$^{-/-}$ CD8$^+$ T cells and normalized to WT CD8$^+$ T cells. Sirius red staining was quantified in liver sections. Mean ± SEM of 1 out of 3 experiments are shown. *$p \leq 0.05$, **$p \leq 0.01$, ns: not significant. Abbreviations: CCasp3, cleaved caspase-3; Mdr2, multidrug resistance protein 2; WT, wild-type.

we treated 6-week-old *Mdr2*$^{-/-}$ mice with an anti-CD8α antibody twice a week for 2 weeks. This resulted in the depletion of hepatic CD8$^+$ T cells, while the number of CD4$^+$ T cells and NK cells were not altered (Figure 2A). In the absence of CD8$^+$ T cells, hepatic NK cells expressed less GzmB, TRAIL, and the degranulation marker CD107a, while expression of the inflammatory cytokine IFNγ was not altered (Figure 2B). In contrast, CD8$^+$ T cells did not affect the phenotype of CD4$^+$ T cells in sclerosing cholangitis (Figure 2C).

Interestingly, liver injury was reduced in the absence of CD8$^+$ T cells (Figure 2D). Cytotoxic lymphocytes induce apoptosis through the activation of caspase-3 in target T cells.[12] We stained for activated caspase-3 (cleaved caspase-3) in liver tissue of *Mdr2*$^{-/-}$ and WT mice. We showed an induction of cleaved caspase-3 in cholangiocytes in sclerosing cholangitis (Supplemental Fig. S1G, http://links.lww.com/HEP/I333), which was reduced after depletion of CD8$^+$ T cells (Figure 2E). Despite not altered expression of α-smooth muscle actin, *Mdr2*$^{-/-}$ mice developed less severe fibrosis after CD8$^+$ T-cell depletion (Figure 2F). Thus, CD8$^+$ T cells aggravated sclerosing cholangitis by supporting cytotoxic NK cells and inducing apoptosis in cholangiocytes.

Reduced cholangiocyte apoptosis and less severe sclerosing cholangitis in the absence of GzmB

After demonstrating the expression of GzmB and TRAIL by CD8$^+$ T cells and NK cells, we assessed the function of both cytotoxic molecules in sclerosing cholangitis. To study the role of GzmB, we generated *Mdr2*$^{-/-}$ × *Gzmb*$^{-/-}$ mice (Supplemental Fig. S3A, http://links.lww.com/HEP/I333) and compared them with *Mdr2*$^{-/-}$ mice. We neither detected *Gzmb* mRNA in liver tissue nor GzmB expression in hepatic T cells and NK cells in 12-week-old *Mdr2*$^{-/-}$ × *Gzmb*$^{-/-}$ mice (Figure 3A). The frequencies of hepatic CD4$^+$ and CD8$^+$ T cells and NK cells were not altered in the absence of GzmB (Figure 3B). We did also not observe an impact of GzmB on the activation of hepatic T cells and NK cells and their expression of TRAIL or IFNγ. Moreover, the IFNγ response, assessed by hepatic mRNA expression of *Ifng*, *Il12b*, and *Cxcl10*, was comparable in *Mdr2*$^{-/-}$ × *Gzmb*$^{-/-}$ and *Mdr2*$^{-/-}$ mice (Supplemental Fig. S3B-E, http://links.lww.com/HEP/I333). However, liver injury (Figure 3C) and induction of cholangiocyte apoptosis were reduced in *Mdr2*$^{-/-}$ × *Gzmb*$^{-/-}$ mice (Figure 3D). In contrast, immune-cell apoptosis did not depend on GzmB (Fig. S3F, http://links.lww.com/HEP/I333). Notably, *Mdr2*$^{-/-}$ × *Gzmb*$^{-/-}$ mice showed attenuated liver fibrosis compared to *Mdr2*$^{-/-}$ mice (Figure 3E). Thus, lymphocyte-derived GzmB induced cholangiocyte apoptosis, thereby aggravating liver injury and fibrosis in sclerosing cholangitis.

Enhanced cytotoxicity and inflammatory cytokine expression in the absence of TRAIL

To investigate the functional role of TRAIL in sclerosing cholangitis, we generated *Mdr2*$^{-/-}$ × *Tnfsf10*$^{-/-}$ mice (Supplemental Fig. S4A, http://links.lww.com/HEP/I333) and compared them with *Mdr2*$^{-/-}$ mice. We confirmed the lack of *Tnfsf10* mRNA in liver tissue and TRAIL expression in hepatic T cells and NK cells in 12-week-old *Mdr2*$^{-/-}$ × *Tnfsf10*$^{-/-}$ mice (Figure 4A). The frequencies of T cells and NK cells were increased in *Mdr2*$^{-/-}$ × *Tnfsf10*$^{-/-}$ mice (Figure 4B). Comparative transcriptome analysis revealed upregulated expression of genes associated with cytotoxicity (*Gzmb*, *Klrk1*, and *Klrd1*), an inflammatory response (*Ifngr1*, *Il12rb2*, and *Tbx21*) and tissue residency (*Itga1* and *Xcl1*) in hepatic CD8$^+$ T_{EM} from *Mdr2*$^{-/-}$ × *Tnfsf10*$^{-/-}$ mice. In contrast, genes associated with T-cell exhaustion (*Tox*, *Pdcd1*, *Ctla4*, *Tigit*, and *Lag3*) were upregulated in CD8$^+$ T_{EM} from *Mdr2*$^{-/-}$ mice. We did not detect differential expression of functionally relevant genes in CD4$^+$ T_{EM} and NK cells (Figure 4C).

Accordingly, hepatic CD8$^+$ T cells were stronger activated and showed increased expression of GzmB and CD107a in sclerosing cholangitis in the absence of TRAIL (Figure 4D). Expression of CD107a and GzmB was also enhanced in CD4$^+$ T cells and NK cells, respectively (Figure 4D), although their activation was not altered (Supplemental Fig. S4B). Together with elevated GzmB levels in culture supernatants of hepatic nonparenchymal cells of *Mdr2*$^{-/-}$ × *Tnfsf10*$^{-/-}$ mice (Supplemental Fig. S4C, http://links.lww.com/HEP/I333), this indicates an enhanced cytotoxic microenvironment in the absence of TRAIL. We further showed elevated IFNγ expression in all lymphocyte subsets and increased *Il12b*, *Ifng,* and *Cxcl10* mRNA expression in liver tissue of *Mdr2*$^{-/-}$ × *Tnfsf10*$^{-/-}$ mice (Figure 4E). Accordingly, the frequency of hepatic DCs expressing IFNγ-inducible MHC-II molecules was elevated (Figure 4E), indicating strengthened DC maturation in *Mdr2*$^{-/-}$ × *Tnfsf10*$^{-/-}$ mice.

Phosphorylation-mediated activation of the signaling molecules zeta chain of T-cell receptor (TCR)-associated protein kinase 70 (ZAP-70) and phospholipase Cγ1 (PLCγ1) is a key step in TCR-induced T-cell activation.[25] We determined increased frequencies of CD8$^+$ T cells with phosphorylated (p)Zap-70 and pPLCγ1, and of CD4$^+$ T cells with pZAP-70 in the livers of *Mdr2*$^{-/-}$ × *Tnfsf10*$^{-/-}$ mice (Figure 4F), demonstrating stronger activation of TCR signaling in sclerosing cholangitis in the absence of TRAIL. We further showed decreased frequencies of Annexin V$^+$ CD4$^+$

and CD8$^+$ T cells in *Mdr2*$^{-/-}$ × *Tnfsf10*$^{-/-}$ mice, indicating TRAIL-dependent T-cell apoptosis in sclerosing cholangitis (Supplemental Fig. S4D, http://links.lww.com/HEP/I333). Taken together, TRAIL regulated T-cell activation and survival as well as lymphocyte cytotoxicity and inflammatory cytokine expression in sclerosing cholangitis.

Lack of TRAIL increased cholangiocyte apoptosis and aggravated sclerosing cholangitis

Since we observed that TRAIL regulates inflammatory and cytotoxic immune responses in sclerosing cholangitis, we wondered whether this might influence liver injury and fibrosis. Indeed, alanine transaminase levels (Figure 5A) and cholangiocyte apoptosis were elevated in *Mdr2*$^{-/-}$ × *Tnfsf10*$^{-/-}$ compared to *Mdr2*$^{-/-}$ mice (Figure 5B). We further showed increased α-smooth muscle actin expression and formation of interportal septa, both indicating myofibroblast expansion in *Mdr2*$^{-/-}$ × *Tnfsf10*$^{-/-}$ mice, together with an exacerbation of hepatic fibrosis in the absence of TRAIL (Figure 5C).

Cholangiocytes proliferate in cholangiopathies, presumably to maintain the biliary structural integrity.[26] We determined CK19-expressing cholangiocytes in sclerosing cholangitis, which expanded from the periportal area to form interportal septa in *Mdr2*$^{-/-}$ × *Tnfsf10*$^{-/-}$ mice (Figure 5D). Accordingly, cholangiocytes expressed the proliferation marker Ki-67 in sclerosing cholangitis (Supplemental Fig. S5, http://links.lww.com/HEP/I333). The lack of TRAIL enhanced Ki-67 expression by cholangiocytes (Figure 5E), whereas we detected reduced expression of Ki-67 in cholangiocytes of *Mdr2*$^{-/-}$ × *Gzmb*$^{-/-}$ mice (Fig. S5, http://links.lww.com/HEP/I333). Activated cholangiocytes have been shown to express pro-inflammatory chemokines, thereby inducing immune-cell recruitment to the liver.[27,28] We detected elevated hepatic expression of the cholangiocyte-associated chemokines[28–30] *Ccl2*, *Cxcl2*, *Cxcl1*, *Ccl4*, *Cxcl16* and *Ccl28* in *Mdr2*$^{-/-}$ × *Tnfsf10*$^{-/-}$ mice (Figure 5F). Thus, TRAIL regulated the progression of liver fibrosis, apoptosis, and proliferation of cholangiocytes, as well as their chemokine expression in sclerosing cholangitis.

TRAIL-deficient CD8$^+$ T cells exacerbated sclerosing cholangitis

After demonstrating a strong inflammatory and cytotoxic phenotype of CD8$^+$ T cells in *Mdr2*$^{-/-}$ × *Tnfsf10*$^{-/-}$ mice, we analyzed the role of CD8$^+$ T-cell–derived TRAIL in sclerosing cholangitis. We transferred CD8$^+$ T cells from *Tnfsf10*$^{-/-}$ or WT mice into 10-week-old *Mdr2*$^{-/-}$ × *Rag1*$^{-/-}$ mice, which lack T and B cells but still harbor NK cells, and analyzed them 8 days later. In the livers of *Mdr2*$^{-/-}$ × *Rag1*$^{-/-}$ mice, transferred *Tnfsf10*$^{-/-}$ CD8$^+$ T cells showed enhanced production of IFNγ and a substantial increase of CD107a compared to WT CD8$^+$ T cells, whereas expression of GzmB was not altered (Figure 6A). Frequencies of endogenous NK cells and their cytotoxic phenotype were not changed after the transfer of *Tnfsf10*$^{-/-}$ CD8$^+$ T cells. However, we determined an elevated expression of IFNγ (Figure 6B). Interestingly, the transfer of TRAIL-deficient CD8$^+$ T cells resulted in more severe liver injury (Figure 6C), elevated cholangiocyte apoptosis and proliferation (Figure 6D, E), and worsened fibrosis in Mdr2$^{-/-}$ × *Rag1*$^{-/-}$ mice (Figure 6F). Thus, CD8$^+$ T-cell–derived TRAIL regulated the inflammatory lymphocyte response and, therefore, liver injury and fibrosis in sclerosing cholangitis.

DISCUSSION

PSC is a life-threatening disease triggered by poorly defined mechanisms. Thus, identifying novel immunopathogenic mechanisms in PSC is of high clinical relevance. In this study, we described the antagonistic effects of GzmB and TRAIL in lymphocyte-mediated cytotoxicity in sclerosing cholangitis.

Immune-cell profiling identified 3 subsets of cytotoxic lymphocytes in sclerosing cholangitis. While CD8$^+$ T_{EM}, CD49b^{hi}, and CD49b^{low} NK cells expressed *Gzmb*, only CD8$^+$ T_{EM} and CD49b^{low} NK cells also expressed *Tnfsf10*. Both showed characteristics of tissue-residing cells, suggesting that these lymphocyte subsets are particularly involved in the pathogenicity of sclerosing cholangitis. We also determined *GZMB*-expressing CD8$^+$ T-cell subsets in human PSC, further indicating the importance of cytotoxic CD8$^+$ T cells for disease pathology. Expansion of CD8$^+$ T cells in juvenile *Mdr2*$^{-/-}$ mice has been correlated with expression of the profibrogenic cytokine osteopontin and liver damage.[31] Together with our finding that CD8$^+$ T-cell depletion ameliorated liver injury in 8 weeks old in *Mdr2*$^{-/-}$ mice, this demonstrates the pathogenicity of CD8$^+$ T cells in early phases of sclerosing cholangitis. Interestingly, NK cells were less cytotoxic in the absence of CD8$^+$ T cells. We have shown that the lack of NK cells attenuated fibrosis in sclerosing cholangitis and reduced the cytotoxicity of CD8$^+$ T cells.[9] This indicates a mutual influence of both lymphocyte subsets supporting their cytotoxicity in sclerosing cholangitis.

Protein expression of GzmB was elevated in hepatic CD8$^+$ T cells and NK cells in *Mdr2*$^{-/-}$ mice, which developed less severe liver injury and fibrosis in the absence of GzmB, associated with reduced cleavage of caspase-3 in cholangiocytes. Immune-cell phenotype and apoptosis were not altered in *Mdr2*$^{-/-}$x*Gzmb*$^{-/-}$ mice, demonstrating that GzmB induced apoptotic cell

death, particularly in liver-resident cells like cholangiocytes, thereby aggravating sclerosing cholangitis. Caspase-3 cleavage in cholangiocytes was also reduced after $CD8^+$ T-cell depletion in *Mdr2*$^{-/-}$ mice, indicating that $CD8^+$ T cells promote cholangiocyte apoptosis by release of GzmB. Accordingly, we have recently described that $CD8^+$ T-cell–derived GzmB induced cleavage of caspase-3 in renal proximal tubular epithelial cells in murine crescentic glomerulonephritis[32] and lupus nephritis.[33]

Several studies describe the importance of TRAIL for T-cell tolerance in liver transplantation[34] and autoimmune diseases.[35] However, the role of TRAIL for immune-cell function in sclerosing cholangitis has not been addressed so far. Our comparative transcriptome analysis revealed TRAIL-dependent differences in the gene expression profile of $CD8^+$ T_{EM}. In the absence of TRAIL, we determined increased expression of *Gzmb* and genes associated with tissue residency in $CD8^+$ T_{EM} in sclerosing cholangitis. In contrast, $CD8^+$ T_{EM} showed elevated expression of marker genes for T-cell exhaustion if TRAIL is expressed. It has been suggested that an exhausted state in $CD8^+$ T cells may be protective in autoimmune disease since exhausted T cells with suppressed but still present effector function could attenuate disease progression.[36] In the absence of TRAIL, this immunoregulation seems to be impaired, which might contribute to aggravated disease pathology in *Mdr2*$^{-/-}$ × *Tnfsf10*$^{-/-}$ mice. Although the gene expression profile of NK cells was not altered, we showed enhanced protein expression of GzmB and IFNγ by $CD8^+$ T cells and NK cells in *Mdr2*$^{-/-}$ × *Tnfsf10*$^{-/-}$ mice. Together with reduced immune-cell apoptosis, this demonstrates that TRAIL regulates lymphocyte survival and their cytotoxic and inflammatory immune responses in sclerosing cholangitis. Our findings are in contrast to acute biliary disease, where TRAIL was shown to promote liver injury.[16–18] The observation that transfer of TRAIL-deficient $CD8^+$ T cells in *Mdr2*$^{-/-}$ × *Rag1*$^{-/-}$ mice resulted in an enhanced IFNγ expression and an aggravated disease pathology indicates that $CD8^+$ T-cell–derived TRAIL controls the pathogenic IFNγ response, which was shown to promote fibrosis in sclerosing cholangitis.[9] Our results are consistent with a study describing elevated IFNγ levels in experimental autoimmune encephalomyelitis (EAE) in the absence of TRAIL.[37] Besides this immunoregulatory function, TRAIL was also shown to reduce fibrosis through NK cell-mediated killing of stellate cells.[38]

Negative co-stimulation might be one mechanism of TRAIL-mediated suppression of T-cell responses in sclerosing cholangitis. It was shown that activation of the TRAIL/DR5 pathway inhibits TCR signaling,[39,40] thereby ameliorating EAE[41] and experimental colitis.[42] Accordingly, we observed enhanced TCR signaling and highly activated and cytotoxic $CD8^+$ T cells in *Mdr2*$^{-/-}$ × *Tnfsf10*$^{-/-}$ mice. Taken together, we provided evidence for an immunoregulatory function of TRAIL in sclerosing cholangitis, which is mediated by inhibition of lymphocyte survival, cytotoxicity, and inflammation.

TRAIL-induced cholangiocyte apoptosis has been described in cholestatic liver disease.[18] However, we demonstrated enhanced cholangiocyte apoptosis in the absence of TRAIL, probably due to increased lymphocyte cytotoxicity. Activated cholangiocytes were found to express chemokines responsible for immune-cell recruitment into the liver.[28,30] Indeed, the expansion of cholangiocytes in *Mdr2*$^{-/-}$ × *Tnfsf10*$^{-/-}$ mice, possibly induced to replenish apoptotic cholangiocytes, was associated with an increased hepatic expression of chemokines, which were shown to be expressed by cholangiocytes of patients with PSC.[29] Thus, enhanced chemokine expression of cholangiocytes might contribute to the amplification of the immune response and the exacerbation of sclerosing cholangitis in the absence of TRAIL.

In conclusion, we have identified GzmB as a mediator of lymphocyte cytotoxicity in sclerosing cholangitis, whereas TRAIL exhibited immunoregulatory properties. Notably, the immunosuppressive effect of TRAIL administration has been demonstrated in preclinical models of inflammation and autoimmune diseases.[41–43] Therefore, both cytotoxic molecules and their downstream signaling pathways could be selectively targeted in future therapeutic strategies for the treatment of autoimmune liver diseases such as PSC.

AUTHOR CONTRIBUTIONS

Mareike Kellerer, Sana Javed, and Laura K. Berkhout: acquisition and analysis of data; Christian Casar, Nico Will, and Dorothee Schwinge: analysis of data; Christian F. Krebs and Christoph Schramm: technical and material support; Katrin Neumann: conception and design, interpretation of data, drafting the article and revising it critically for important intellectual content, and final approval of the version to be published; Gisa Tiegs: conception and design of research, study supervision, interpretation of data, drafting the article and revising it critically for important intellectual content, final approval of the version to be published, obtained funding.

ACKNOWLEDGMENTS

The authors thank Elena Tasika, Carsten Rothkegel, and the co-workers of the FACS and single-cell Core Units at the University Medical Center, Hamburg-Eppendorf, for their excellent technical assistance.

FUNDING INFORMATION

This work was supported by the Deutsche Forschungsgemeinschaft (DFG): Clinical Research Unit 306 'Primary Sclerosing Cholangitis' project 4 to Gisa Tiegs.

CONFLICTS OF INTEREST

Christoph Schramm consults for Agomab and Chemomab. He advises Pliant. He received grants from Falk and Roche. The remaining authors have no conflicts to report.

REFERENCES

1. Lazaridis KN, LaRusso NF. Primary sclerosing cholangitis. N Engl J Med. 2016;375:1161–70.
2. Liu JZ, Hov JR, Folseraas T, Ellinghaus E, Rushbrook SM, Doncheva NT, et al. Dense genotyping of immune-related disease regions identifies nine new risk loci for primary sclerosing cholangitis. Nat Genet. 2013;45:670–5.
3. Karlsen TH, Boberg KM, Olsson M, Sun JY, Senitzer D, Bergquist A, et al. Particular genetic variants of ligands for natural killer cell receptors may contribute to the HLA associated risk of primary sclerosing cholangitis. J Hepatol. 2007;46: 899–906.
4. Liaskou E, Jeffery LE, Trivedi PJ, Reynolds GM, Suresh S, Bruns T, et al. Loss of CD28 expression by liver-infiltrating T cells contributes to pathogenesis of primary sclerosing cholangitis. Gastroenterology. 2014;147:221–232.e7.
5. Kunzmann LK, Schoknecht T, Poch T, Henze L, Stein S, Kriz M, et al. Monocytes as potential mediators of pathogen-induced T-helper 17 differentiation in patients with primary sclerosing cholangitis (PSC). Hepatology. 2020;72:1310–26.
6. Poch T, Krause J, Casar C, Liwinski T, Glau L, Kaufmann M, et al. Single-cell atlas of hepatic T cells reveals expansion of liver-resident naive-like CD4+ T cells in primary sclerosing cholangitis. J Hepatol. 2021;75:414–23.
7. Gravano DM, Hoyer KK. Promotion and prevention of autoimmune disease by CD8+ T cells. J Autoimmun. 2013; 45:68–79.
8. Fickert P, Pollheimer MJ, Beuers U, Lackner C, Hirschfield G, Housset C, et al. Characterization of animal models for primary sclerosing cholangitis (PSC). J Hepatol. 2014;60:1290–303.
9. Ravichandran G, Neumann K, Berkhout LK, Weidemann S, Langeneckert AE, Schwinge D, et al. Interferon-γ-dependent immune responses contribute to the pathogenesis of sclerosing cholangitis in mice. J Hepatol. 2019;71:773–82.
10. Zhu C, Boucheron N, Müller AC, Májek P, Claudel T, Halilbasic E, et al. 24-Norursodeoxycholic acid reshapes immunometabolism in CD8+ T cells and alleviates hepatic inflammation. J Hepatol. 2021;75:1164–76.
11. Barry M, Bleackley RC. Cytotoxic T lymphocytes: all roads lead to death. Nat Rev Immunol. 2002;2:401–9.
12. Bleackley RC. A molecular view of cytotoxic T lymphocyte induced killing. Biochem Cell Biol. 2005;83:747–51.
13. Li Y, Li B, You Z, Zhang J, Wei Y, Li Y, et al. Cytotoxic KLRG1 expressing lymphocytes invade portal tracts in primary biliary cholangitis. J Autoimmun. 2019;103:102293.
14. Cardoso Alves L, Corazza N, Micheau O, Krebs P. The multifaceted role of TRAIL signaling in cancer and immunity. FEBS J. 2021;288:5530–54.
15. Beyer K, Baukloh AK, Stoyanova A, Kamphues C, Sattler A, Kotsch K. Interactions of tumor necrosis factor-related apoptosis-inducing ligand (TRAIL) with the immune system: Implications for inflammation and cancer. Cancers (Basel). 2019; 11:1161.
16. Zheng SJ, Wang P, Tsabary G, Chen YH. Critical roles of TRAIL in hepatic cell death and hepatic inflammation. J Clin Invest. 2004;113:58–64.
17. Kahraman A, Barreyro FJ, Bronk SF, Werneburg NW, Mott JL, Akazawa Y, et al. TRAIL mediates liver injury by the innate immune system in the bile duct-ligated mouse. Hepatology. 2008;47:1317–30.
18. Takeda K, Kojima Y, Ikejima K, Harada K, Yamashina S, Okumura K, et al. Death receptor 5 mediated-apoptosis contributes to cholestatic liver disease. Proc Natl Acad Sci U S A. 2008;105:10895–900.
19. Guicciardi ME, Krishnan A, Bronk SF, Hirsova P, Griffith TS, Gores GJ. Biliary tract instillation of a SMAC mimetic induces TRAIL-dependent acute sclerosing cholangitis-like injury in mice. Cell Death Dis. 2017;8:e2535.
20. Krishnan A, Katsumi T, Guicciardi ME, Azad AI, Ozturk NB, Trussoni CE, et al. Tumor necrosis factor-related apoptosis-inducing ligand receptor deficiency promotes the ductular reaction, macrophage accumulation, and hepatic fibrosis in the Abcb4-/- Mouse. Am J Pathol. 2020;190:1284–97.
21. Fleming SJ, Chaffin MD, Arduini A, Akkad AD, Banks E, Marioni JC, et al. Unsupervised removal of systematic background noise from droplet-based single-cell experiments using Cell Bender. Nat Methods. 2023;20:1323–35.
22. Bernstein NJ, Fong NL, Lam I, Roy MA, Hendrickson DG, Kelley DR. Solo: doublet identification in single-cell RNA-Seq via semi-supervised deep learning. Cell Syst. 2020;11:95–101.e5.
23. Stuart T, Butler A, Hoffman P, Hafemeister C, Papalexi E, Mauck WM 3rd, et al. Comprehensive integration of single-cell data. Cell. 2019;177:1888–1902.e21.
24. Squair JW, Gautier M, Kathe C, Anderson MA, James ND, Hutson TH, et al. Confronting false discoveries in single-cell differential expression. Nat Commun. 2021;12:5692.
25. Gaud G, Lesourne R, Love PE. Regulatory mechanisms in T cell receptor signalling. Nat Rev Immunol. 2018;18:485–97.
26. O'Hara SP, Tabibian JH, Splinter PL, LaRusso NF. The dynamic biliary epithelia: molecules, pathways, and disease. J Hepatol. 2013;58:575–82.
27. Banales JM, Huebert RC, Karlsen T, Strazzabosco M, LaRusso NF, Gores GJ. Cholangiocyte pathobiology. Nat Rev Gastroenterol Hepatol. 2019;16:269–81.
28. Reich M, Spomer L, Klindt C, Fuchs K, Stindt J, Deutschmann K, et al. Downregulation of TGR5 (GPBAR1) in biliary epithelial cells contributes to the pathogenesis of sclerosing cholangitis. J Hepatol. 2021;75:634–46.
29. Tabibian JH, Trussoni CE, O'Hara SP, Splinter PL, Heimbach JK, LaRusso NF. Characterization of cultured cholangiocytes isolated from livers of patients with primary sclerosing cholangitis. Lab Invest. 2014;94:1126–33.
30. Borchers AT, Shimoda S, Bowlus C, Keen CL, Gershwin ME. Lymphocyte recruitment and homing to the liver in primary biliary cirrhosis and primary sclerosing cholangitis. Semin Immunopathol. 2009;31:309–22.
31. Taylor AE, Carey AN, Kudira R, Lages CS, Shi T, Lam S, et al. Interleukin 2 promotes hepatic regulatory T cell responses and protects from biliary fibrosis in murine sclerosing cholangitis. Hepatology. 2018;68:1905–21.
32. Mueller A, Zhao Y, Cicek H, Paust HJ, sivayoganathan a, linke a, et al. transcriptional and Clonal Characterization of Cytotoxic T cells in crescentic glomerulonephritis. J Am Soc Nephrol. 2023; 34:1003–18.
33. Linke A, Cicek H, Müller A, Meyer-Schwesinger C, Melderis S, Wiech T, et al. Antigen Cross-presentation by murine proximal tubular epithelial cells induces cytotoxic and inflammatory CD8+ T Cells. Cells. 2022;11:1510.
34. Harmon C, Sanchez-Fueyo A, O'Farrelly C, Houlihan DD. Natural killer cells and liver transplantation: orchestrators of rejection or tolerance? Am J Transplant. 2016;16:751–7.
35. Rossin A, Miloro G, Hueber AO. TRAIL and FasL functions in cancer and autoimmune diseases: towards an increasing complexity. Cancers (Basel). 2019;11:639.
36. Collier JL, Weiss SA, Pauken KE, Sen DR, Sharpe AH. Not-so-opposite ends of the spectrum: CD8+ T cell dysfunction across chronic infection, cancer and autoimmunity. Nat Immunol. 2021; 22:809–19.

37. Ikeda T, Hirata S, Fukushima S, Matsunaga Y, Ito T, Uchino M, et al. Dual effects of TRAIL in suppression of autoimmunity: the inhibition of Th1 cells and the promotion of regulatory T cells. J Immunol. 2010;185:5259–67.
38. Radaeva S, Sun R, Jaruga B, Nguyen VT, Tian Z, Gao B. Natural killer cells ameliorate liver fibrosis by killing activated stellate cells in NKG2D-dependent and tumor necrosis factor-related apoptosis-inducing ligand-dependent manners. Gastroenterology. 2006;130:435–52.
39. Lehnert C, Weiswange M, Jeremias I, Bayer C, Grunert M, Debatin KM, et al. TRAIL-receptor costimulation inhibits proximal TCR signaling and suppresses human T cell activation and proliferation. J Immunol. 2014;193:4021–31.
40. Lünemann JD, Waiczies S, Ehrlich S, Wendling U, Seeger B, Kamradt T, et al. Death ligand TRAIL induces no apoptosis but inhibits activation of human (auto)antigen-specific T cells. J Immunol. 2002;168:4881–8.
41. Chyuan IT, Tsai HF, Wu CS, Sung CC, Hsu PN. TRAIL-Mediated suppression of T Cell receptor signaling inhibits T Cell activation and inflammation in experimental autoimmune encephalomyelitis. Front Immunol. 2018;9:15.
42. Chyuan IT, Tsai HF, Wu CS, Hsu PN. TRAIL suppresses gut inflammation and inhibits colitogeic T-cell activation in experimental colitis via an apoptosis-independent pathway. Mucosal Immunol. 2019;12:980–9.
43. Song K, Chen Y, Göke R, Wilmen A, Seidel C, Göke A, et al. Tumor necrosis factor-related apoptosis-inducing ligand (TRAIL) is an inhibitor of autoimmune inflammation and cell cycle progression. J Exp Med. 2000;191:1095–104.

How to cite this article: Kellerer M, Javed S, Casar C, Will N, Berkhout LK, Schwinge D, et al. Antagonistic effects of the cytotoxic molecules granzyme B and TRAIL in the immunopathogenesis of sclerosing cholangitis. Hepatology. 2024;80:844–858. https://doi.org/10.1097/HEP.0000000000000830